Biochimica et Biophysica Acta 894 (1987) 91–107
Elsevier

BBA 42629

Optical-difference spectra of the S-state transitions in the photosynthetic oxygen-evolving complex

Jérôme Lavergne

Institut de Biologie Physico-Chimique, Paris (France)

(Received 6 March 1987)

Key words: Photosystem II; Oxygen-evolving complex; Manganese; Cytochrome *b*-559; S state transition; Spectroscopy, difference

A deconvolution of the difference spectra (in the near-ultraviolet and visible regions) associated with the successive oxidation steps of the oxygen-evolving complex is presented. The experimental procedure was designed to eliminate any contribution from the secondary quinone acceptor Q_B and to obtain contrasted sequences with respect to the initial distribution of the S_0/S_1 states. Both conditions were obtained by using various preillumination procedures in the presence of a low concentration of carbonylcyanide *p*-trifluoromethoxyphenylhydrazone (FCCP). This substance accelerates the deactivation of states S_2 and S_3 without affecting the redox state of the two-electron gate Q_B, so that the steady-state equipartition of Q_B and Q_B^- reached through a continuous preillumination is left undisturbed during the deactivation of the S-states. Only a small absorption change is associated with the $S_0 \rightarrow S_1$ transition in the spectral region investigated. The spectrum of the $S_1 \rightarrow S_2$ transition consists of a broad band peaking around 315 nm and a chlorophyll *a* bandshift in the blue region. The bandshift is mostly absent from the spectrum of $S_2 \rightarrow S_3$ which also differs slightly from that of $S_1 \rightarrow S_2$ in the ultraviolet with a smaller band peaking around 305 nm. These results are consistent with – but do not ascertain – a manganese oxidation Mn (III → IV) occurring on the two latter steps. The weakness of the $S_0 \rightarrow S_1$ spectrum may suggest that manganese is not involved at this step, although an Mn (II → III) oxidation cannot be ruled out. An additional spectral component occurs upon the first flash of the sequences. The spectrum of this slow turnover signal is presented and discussed.

Introduction

Whereas the essential knowledge about the process of water oxidation in photosynthesis was long contained in the formal scheme of Kok [1], a wealth of experimental information based on different techniques has appeared in the recent period, accompanied with – conflicting – tentative models of the molecular mechanisms that could be involved in this process (see Refs. 2 and 3 for reviews). According to Kok's scheme, the oxygen-evolving complex goes over a cycle of five oxidation states:

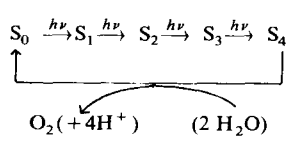

Abbreviations: PS, Photosystem; FCCP, carbonylcyanide *p*-trifluoromethoxyphenylhydrazone; DCMU, 3-(3,4-dichlorophenyl)-1,1-dimethylurea; Tricine, *N*-[2-hydroxy-1,1-bis(hydroxymethyl)ethyl]glycine; Chl, chlorophyll.

Correspondence: J. Lavergne, Institut de Biologie Physico-Chimique, 13, rue Pierre et Marie Curie, 75005 Paris, France.

where each $\xrightarrow{h\nu}$ arrow denotes the abstraction of one electron driven by a photochemical turnover of PS II. S_4 is a transient state decaying in the millisecond range with concomitant release of molecular oxygen. States S_3 and S_2 deactivate towards S_1 in the tens of seconds time-range, whereas S_0 and S_1 are stable in the dark. The usual distribution found in dark-adapted material is about 25% for S_0 and 75% for S_1, but may substantially vary depending on dark-adaption time [4], pH [5], redox potential [6], or preillumination [1]. Upon illumination with a saturating short flash, a one-step advance in the cycle is obtained, except for randomly distributed fractions of misses ($\alpha \simeq 10\%$) and double-hits ($\beta \simeq 5\%$), when using xenon flashes of a few microsecond duration.

A significant advance towards a more detailed description of the water-oxidation mechanism came from Fowler's work [7] who reported that the four protons involved in the overall reaction are not all released in the final, oxygen-evolving step $S_4 \rightarrow S_0$, but only two of them; one accompanying the $S_0 \rightarrow S_1$ step and the other the $S_2 \rightarrow S_3$ step. This 1,0,1,2-pattern for proton release was controversial for some time, but confirmed by Saphon and Crofts [8], and later accepted by Förster and Junge [9].

Four manganese atoms are known to be required in the functional oxygen-evolving complex (see review Ref. 2), and clear evidence for their actual involvement in oxidant accumulation came from the discovery of the 'multiline' ESR signal by Dismukes and Siderer [10]. This signal is observed after freezing preilluminated samples close to liquid helium temperatures, and was shown to accompany uniquely state S_2. The ESR spectrum was interpreted by Dismukes and Siderer as arising from a dinuclear (or possibly tetranuclear) mixed-valence Mn complex, such as Mn_2(III, IV).

Further information on the oxidation states of the oxygen-evolving complex can be obtained from optical absorption changes. Such S-states-related changes were reported in the near ultraviolet and blue regions of the spectrum [11–13], in the red region [14] and in the infrared [15]. Analyzing the ultraviolet absorption changes, Dekker et al. [13] proposed that an identical spectral change was occurring upon each of the first three oxidation steps ($S_0 \rightarrow S_1$, $S_1 \rightarrow S_2$, $S_2 \rightarrow S_3$), with a decay of the cumulated signal during the $S_3 \rightarrow (S_4 \rightarrow) S_0$ step. They further pointed out some similarity between this spectrum and that reported for the Mn(IV)-minus-Mn(III) difference spectrum in synthetic manganese gluconate compounds [16]. The authors thus proposed that three Mn(III) atoms were successively oxidized to Mn(IV) upon each of the transitions from S_0 to S_3.

In a previous paper [17], I re-examined this problem. One main difficulty in this spectral region is to extract the S-related signal from other contributions such as the semiquinone signal arising from the two-electron gate behaviour of the secondary quinonic acceptor, Q_B, of PS II. I did not tackle at that time the problem of spectral deconvolution, but merely accepted Dekker et al's report of a single spectral change associated with the S-state oxidations. The stoichiometric aspect of the problem can thus be easily submitted to experimental testing by working at a wavelength (295 nm) that is isobestic for the semiquinone signal, but almost maximum for the S-related signal. The reason for questioning the 1,1,1,−3 stoichiometry proposed by Dekker et al. was that their data could be fitted as satisfactorily with other patterns relating the spectral change to the S states, namely that (0,1,0,−1) previously proposed by Velthuys [12]. The problem is not primarily the accuracy of these data, but rather their discriminative power. Most of the information is contained in the first few flashes, when the S-state distribution is significantly unbalanced. Unfortunately, as will be discussed in the present paper, an additional absorption change occurs on the first flash, which may lead to discarding the first flash data, as did Dekker et al., or at least, to complicate the the procedure by which information is retrieved from them. Nevertheless, it is possible to compare experiments where some of Kok's parameters are modified, e.g., by using suitable preillumination procedures, and to test whether the experimental response is better predicted by such or such model. This semi-qualitative analysis was done in Ref. 17, and the results showed that the $S_0 \rightarrow S_1$ and the $S_2 \rightarrow S_3$ transitions both gave a smaller contribution (if any) than the $S_1 \rightarrow S_2$ transition to the absorption change at 295 nm. If a choice had to be made

between 1,1,1,−3 and 0,1,0,−1 models, then both these features gave advantage to the latter.

In the present paper, one shows that a preillumination with continuous light can totally eliminate the Q_B/Q_B^- signal in algae to which an ADRY [18] substance (FCCP) has been added. This increases considerably the accuracy to which a deconvolution of the individual spectral contributions of each S-transition can be obtained. The picture that emerges from this work is that in the spectral domain investigated (290–560 nm), little or no absorption change is associated with the $S_0 \rightarrow S_1$ transition, and that the two other transitions ($S_1 \rightarrow S_2$ and $S_2 \rightarrow S_3$) have spectra that significantly differ from each other. These findings lead to the conclusion that the substance which goes oxidized in the $S_0 \rightarrow S_1$ step is of a different nature from those involved in the other transitions, and may not be a manganese. On the other hand, the partial similarity of the spectra of $S_1 \rightarrow S_2$ and $S_2 \rightarrow S_3$ suggests that a manganese oxidation is probably occurring in both these steps.

Materials and Methods

The photosynthetic material consisted of whole cells of a double mutant, S56, of the green alga *Chiorella sorokiniana*. This strain (isolated by P. Bennoun) is devoid of PS I centers and lacks part of the light-harvesting pigment protein complex. Structural and biochemical information about *C. sorokiniana* mutant strains may be found in Ref. 19, and previous investigations of PS II absorption changes in S56 were reported in Refs. 20, 21 and 17. Before being used in the experiments, the algal culture was incubated for 5 min with $2 \cdot 10^{-4}$ M benzoquinone, then rapidly pelleted, washed once in 50 mM Tricine (pH 7.5), KCl 50 mM medium, centrifuged again, and finally resuspended in 50 mM phosphate buffer (pH 6.5) with 10% ficoll. The algae were used at a concentration of about 20 μg Chl/ml (one should remember that the centers/Chl ratio is higher in this strain due to the partial pigment deficiency). The ionophore dicyclohexyl-18-crown-6 [22] was added to the suspension medium at a concentration of $3 \cdot 10^{-4}$ M, so that the field-indicating absorption change had completely decayed at 50 ms after an actinic flash. The quinone treatment brings about a stably oxidized plastoquinone pool in the dark and a normal pattern of oxygen evolution during the first ten flashes of a series with no need for artificial acceptor addition. All the experiments were run by admitting a fresh sample (cuvette volume, 2 ml) from a 150 ml suspension stirred in the dark, into which it was recycled after the measurement.

Absorption changes were measured with the apparatus described in Refs. 23 and 24, using monochromatic flashes (2 μs duration) as a detecting beam. Saturating actinic flashes were obtained from another Xe flashlamp (2 μs duration at half pulse height) with a broad-band blue filter. The optical path length was 16 mm, the spectral band width ranging from about 5 nm in the ultraviolet to about 1 nm in the green region.

For the acquisition of the spectral data, a total of 8–16 experiments was averaged at each wavelength, scanning the spectral domain investigated first in one direction and then back: this gave a check that no large evolution of the material had occurred (in which case the experiment was discarded) and allowed a correction for minor drifts (the washing step following the quinone treatment was found to improve the stability of the material). Methods used for deconvolution of the spectra associated with the individual S-transitions will be discussed in the next section and in the appendices.

Results

Effects of FCCP

As stated in the introduction, the main difficulty in studying the S-related absorption changes in the ultraviolet is to eliminate the contamination from the signal associated with the secondary acceptor Q_B. The problem is that this signal is rather large in this region, and, besides, behaves in a periodic manner during the flash sequence (period of two flashes), which makes its deconvolution from the four-flash periodic change associated with the S-states quite tricky. It is possible to eliminate the Q_B change by preilluminating the sample until a steady state is reached where half the centers are in the semiquinone form Q_B^-. Such a preillumination, however, also gives a steady-state equidistribution of the S-states. Since the

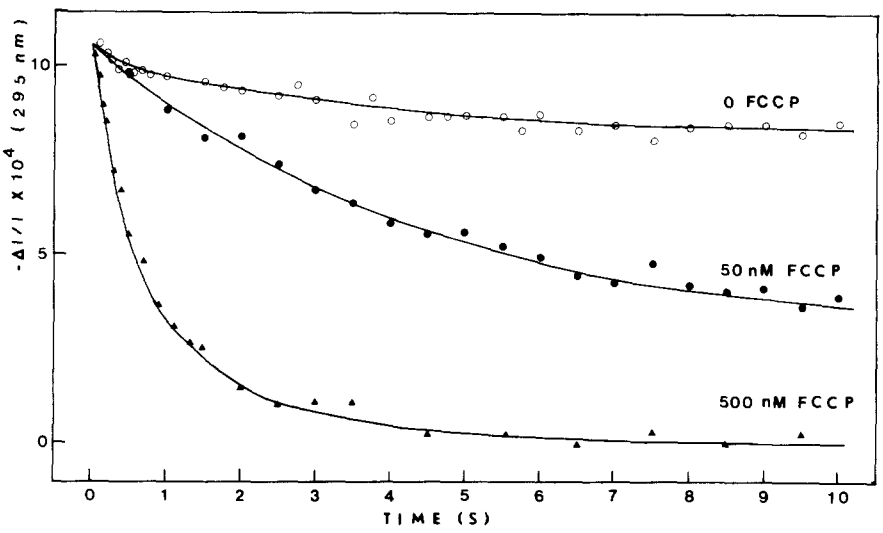

Fig. 1. Kinetics of the absorption change at 295 nm following a saturating flash, in the presence of various concentrations of FCCP, as indicated.

dark re-reduction of S_2 and S_3 involves a recombination with Q_B^- [25], some coupling between the S and Q_B states is again expected after a deactivation period. If it were possible to deactivate the S-states without involving the Q_B^- electron, one could obtain an unbalance of the S distribution without affecting the equidistribution of Q_B/Q_B^-. This proved to be possible by using FCCP, an 'ADRY' reagent [18], i.e., a substance that accelerates the dark deactivation of states S_2 and S_3.

Fig. 1 shows the effect of FCCP on the decay of the absorption change induced by a flash at 295 nm. This wavelength is isobestic for the $Q_B^- - Q_B$ difference spectrum, and the major contribution is the change associated with the $S_1 \rightarrow S_2$ transition. In the absence of FCCP, the decay is very slow, with a half-time of several tens of seconds, except for a small faster phase in the hundreds ms range (in similar experiments, however, this fast phase was sometimes found significantly larger than in the experiment shown in Fig. 1). In the presence of 50 nM FCCP, the half-time becomes about 5 s,

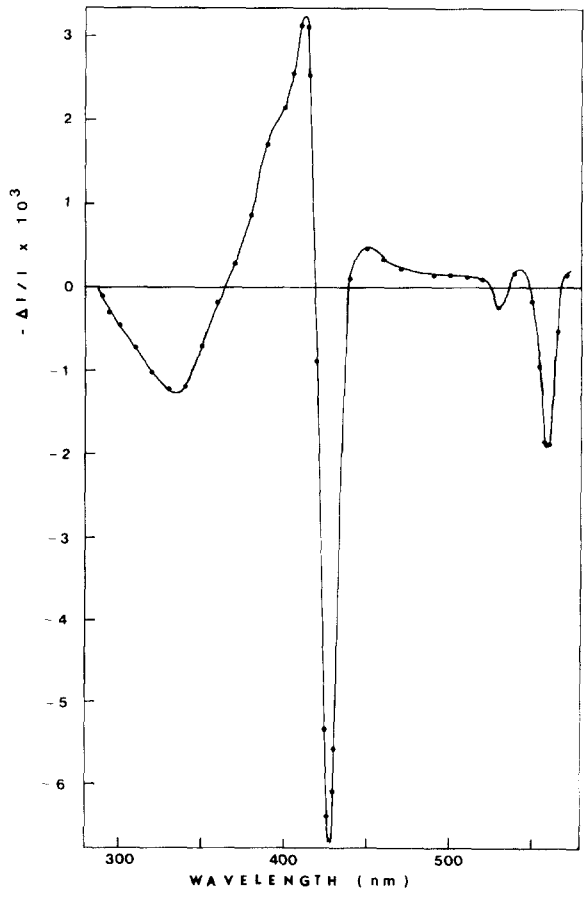

Fig. 2. Spectrum of oxidized-reduced cytochrome *b*-559 obtained by plotting the absorption changes monitored 2 s after a saturating flash preceded by a 1 s preillumination with continuous light and 20 s darkness, in the presence of 10 μM FCCP.

and 500 ms with 500 nM FCCP. This shows that FCCP penetrates the algae, and causes acceleration of S_2 re-reduction, consistently with the mobile catalyst action found for other ADRY's [26]. When repeating the experiment of Fig. 1 using a group of two closely spaced flashes (not shown) instead of a single flash, similar or slightly faster decay rates were observed. As will be shown below, the absorption change under such conditions contains a noticeable contribution from the $S_2 \rightarrow S_3$ transition. Thus the time-course of the FCCP-accelerated S_3 re-reduction is similar with, or slightly faster than, that of S_2.

It has been reported therefore [27] that FCCP causes a photo-oxidation of cytochrome *b*-559. Such a photo-oxidation was readily observed under our experimental conditions, as shown in Fig. 2. This is a plot of the absorption change monitored 2 s after a flash on a sample that was dark-adapted for 20 s following a 1 s preillumination with continuous light, in the presence of 10 μM FCCP. The preillumination procedure, as will be shown below, eliminates the contribution from the Q_B/Q_B^- system, so that the spectrum of Fig. 2 is presumably a pure oxidized – reduced spectrum of cytochrome *b*-559. The major differences with the spectrum reported by Garewal and Wasserman [28], e.g., a lower Soret-to-alpha ratio, are due to the flattening effect [29] in regions where the background absorbance of the algae is high. On the other hand, a difference in the base-line position above 440 nm is also observed. The extent of cytochrome photooxidation obtained in this figure accounts for about 75–80% of that observed when using a fully dark-adapted sample, because the preillumination caused oxidation of all the photo-oxidizable cytochrome, and the 20 s dark period did not allow a total re-reduction. The half-time for this re-reduction (not shown) was about 10 s. It is beyond our present scope to give a detailed account of this subject, but the following point is still worth mentioning, for which experimental support will be given elsewhere. The time-course of cytochrome oxidation is similar with that of S_2, or S_3 (when a group of two closely spaced flashes is used), re-reduction, in the presence of various concentrations of FCCP. However, even when the cytochrome is fully photo-oxidized, the accelerated deactivation of S_2 (or S_3) still proceeds at the same rate. Thus the cytochrome oxidation is a by-product of the FCCP-induced re-reduction of the higher S-states, and the amount of oxidizable cytochrome does not control the deactivation.

We now come to the central point of the elimination of the secondary acceptor absorption changes by a preillumination in the presence of FCCP. Fig. 3 is a plot of the absorption changes monitored at 320 nm (close to the peak of the $Q_B^- - Q_B$ difference spectrum), 50 ms after each flash of a series. FCCP was present at a concentration of 500 nM, so that the S_2 or S_3 deactivation is small during the 100 ms spacing between the flashes of the series, but total during the 10 s dark time allowed after the various preillumination procedures (see Fig. 1). In part A, the preilluminations were zero, one, or two flashes fired 10 s apart, with again 10 s darkness before the flash series. In part B, the same procedures were used but preceded by a 3 s preillumination with continuous light, followed by 10 s darkness. The results can be interpreted as follows. The

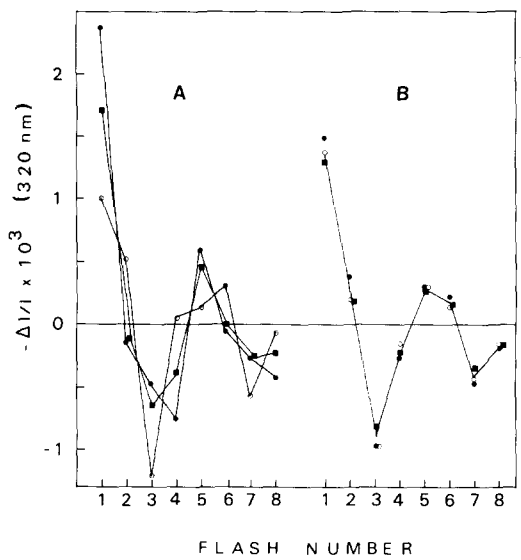

Fig. 3. Sequences of the absorption changes at 320 nm during a series of saturating flashes, spaced 100 ms apart, in the presence of FCCP 500 nM. The change induced by each flash was measured 50 ms after the flash. In A, the dark-adapted sample was preilluminated with 0 (●), 1 (○), or 2 (■) flashes spaced 10 s apart, and a 10 s deactivation period was allowed before the flash series. In B, a 3 s continuous preillumination followed by 10 s darkness preceded the flash preilluminations.

TABLE I

SEQUENCES OF THE ABSORPTION CHANGES AT 320 nm RECORDED 50 ms AFTER EACH FLASH OF A SERIES (SPACED 51 ms APART), IN THE PRESENCE OF 500 nM FCCP

Preilluminations: 1 s with continuous light, 20 s darkness, one or two flashes as indicated, and again 20 s darkness. Each sequence is the average of ten experiments. The standard deviation computed for these data from that obtained on the baselines is ±10.

		$10^6 \cdot \frac{-\Delta I}{I}$							
		Flash number							
		1	2	3	4	5	6	7	8
1s continuous light	+1F	1272	445	−1089	−124	345	305	−348	−83
	+2F	1285	442	−1058	−141	360	289	−351	−94

centers which are promoted to state S_2 by a preillumination flash fully deactivate to S_1 during the 10 s dark period, so that the initial distribution of the S states when the flash series is triggered is about 100% S_1, except in the zero flash preillumination case where some S_0 may also be present. Thus the large variations depending on the number of preillumination flashes in Fig. 3A result from the superimposition of preillumination-dependent signals to basically identical S-sequences. It is readily seen that this variable contribution has the characteristic binary behaviour of the Q_B^-/Q_B two electron gate. The period-2 contribution is completely wiped out in the experiment of Fig. 3B, where the continuous preillumination caused a stable equipartition of states Q_B and Q_B^-. FCCP thus succeeds in uncoupling the Q_B system from the S-system, a finding that will considerably facilitate the deconvolution of the S-related absorption changes. In order to substantiate this point further which is of critical importance to appreciate the significance of the deconvolutions described in the following sections, Table I shows another set of data for a similar experiment. These were obtained under precisely the same conditions as the experiments used for the deconvolutions, i.e., a shorter illumination time (1 s) with a higher intensity, and dark times of 20 s (instead of 10 s in Fig. 3). More signal averaging was carried out in order to improve the signal-to-noise ratio. As may be seen, the sequences after one or two preillumination flashes are identical within the experimental accuracy, which proves, on the one hand, that the contribution from Q_B/Q_B^- is totally canceled, and, on the other hand, that the dark interval of 20 s is

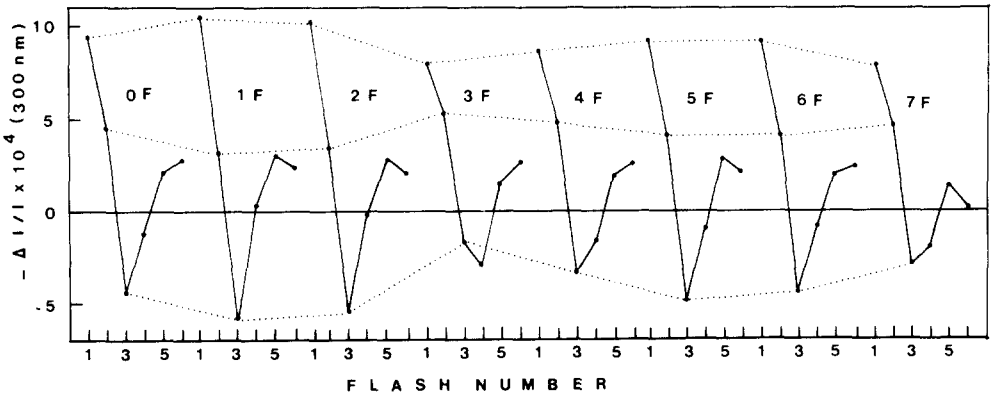

Fig. 4. Sequences of the absorption change at 300 nm during a series of saturating flashes, following various preilluminations in the presence of 500 nM FCCP. The absorption increment was measured 50 ms after each flash (spaced 100 ms apart). The preillumination consisted of 1 s continuous light, 15 s darkness, a group of 0–7 saturating flashes as indicated (spaced 100 ms apart), and another 15 s dark period before running the flash series. The dotted lines join the first, second, and third flashes of the sequences.

sufficient for a complete deactivation towards state S_1. All the experiments reported in the following were run in the presence of FCCP (500 nM), using preillumination with continuous light to eliminate contamination from the secondary acceptor. In the absence of preillumination (not shown), almost identical ultraviolet absorption change sequences were obtained in the presence and in the absence of FCCP (with superimposed contributions from the S- and Q_B-systems), provided the flashing frequency was high compared with the deactivation rate. We generally used 50 ms intervals with 500 nM FCCP, which satisfies the above condition. However, in the spectral regions close to the peaks of the cytochrome, its photo-oxidation in a few percent of the centers causes significant signals that may require correction. Actually, for a better accuracy of the deconvolutions, we subtracted the cytochrome contribution in the whole spectral range investigated, as will be indicated.

Direct evidence showing that the change associated with S_0-S_1 transition is small

This assertion will be established on a quantitative basis as a result of the deconvolution procedures described in the following sections. However, since it is a major point in the controversy with other authors [13,30], it is worthwhile to substantiate it with more direct, semi-qualitative evidence. Fig. 4 shows the sequences of the absorption changes monitored 50 ms after each flash at 300 nm. Following a 1 s continuous preillumination and a dark period of 15 s to ensure total deactivation of S_2 and S_3, a group of 0–7 closely spaced preillumination flashes were fired, again followed by 15 s darkness before recording the sequence. Since states S_2 and S_3 deactivate towards S_1, whereas S_0 and S_1 remain stable in the dark (at least in the relevant time-range for this experiment), the sequences of Fig. 4 should only differ through the initial S_0/S_1 distribution. One expects this ratio to be 25%/75% in the zero flash sequence (because of the continuous preillumination), close to 0/1 after one or two preillumination flashes, and about 50%/50% or so after three flashes. The proportion of S_0 should again decrease after five or six preillumination flashes, and increase again after seven flashes. It turns out that the absorption change monitored after the first flash of the sequence follows the S_1/S_0 distribution, showing a minimum whenever S_0 is maximum. The various patterns of sequences obtained depending on the preillumination are consistent with the predictions given above as to the initial distribution. For instance, the amplitude of the negative change after the third flash, which mostly reflects the $S_3 \rightarrow S_0$ transition, is larger when the initial concentration of S_1 is expected to be large. It may also be seen that the preillumination dependence described for the first flash is still observed for the fifth flash, where, in spite of the damping, some recurrence of the initial distribution is expected.

These findings provide a strong clue that, at 300 nm, the absorption change associated with the $S_0 \rightarrow S_1$ transition is significantly smaller than that of the $S_1 \rightarrow S_2$ transition. Similar experiments (see Fig. 6) showed this to be true in the whole spectral range from 290 nm to 390 nm. This conclusion is not affected by the possible presence of an additional spectral contribution to the change monitored after the first flash. Indeed, as will be shown in the following, such a contribution does occur. However, the period-4 oscillatory behaviour of the first flash signal with respect to the number of preilluminating flashes clearly identifies the S-state nature of the phenomenon. An experiment similar with that of Fig. 4, but run in the absence of FCCP, was originally reported in Ref. 17, yielding similar results – and conclusion. To assess more quantitatively how much smaller the $S_0 \rightarrow S_1$ change is, compared with the $S_1 \rightarrow S_2$ absorption change, obviously requires a precise deconvolution as will be next described. Nevertheless, the qualitative view that readily emerges from such experiments clearly rules out proposed models where both absorption changes are identical [13], or where the $S_0 \rightarrow S_1$ contribution is even larger than that of $S_1 \rightarrow S_2$ (at 300 nm) [30].

Obtainment of the spectral data

Fig. 5 gives an example of the raw material which was used for deconvolution of the spectra of the successive S transitions. At each wavelength, three experiments (A, B and C) were successively run. In A, a fresh sample was submitted to the 1 s continuous illumination, and a

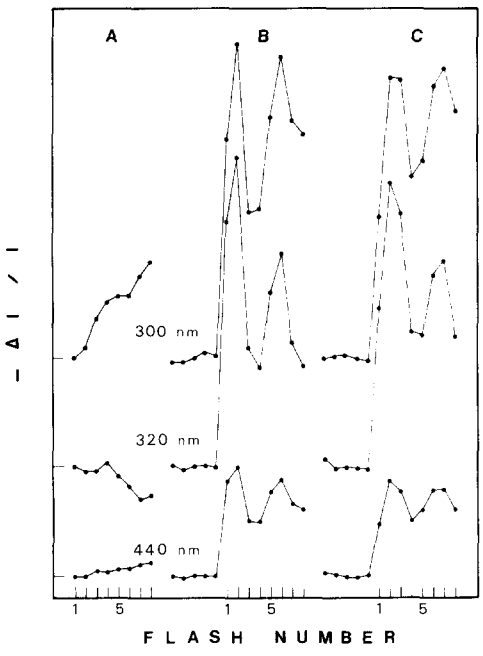

Fig. 5. A plot of the raw data used for deconvolution, at 300 nm, 320 nm and 440 nm, as indicated. In (A) the sequence is run immediately after the 1 s continuous illumination. In (B) one preillumination flash was fired 20 s after the continuous illumination, and 20 s before running the sequence. The same procedure was used in (C), followed by an additional group of three flashes (50 ms apart), and 20 s dark interval before the measuring sequence. Other details given in the text.

series of eight flashes (spaced 51 ms apart) triggered immediately after the offset of the continuous beam. The pulses of detecting light at a given wavelength monitor the absorbance immediately before the first flash and at 50 ms after each flash of the series. The measured values were plotted for three wavelengths (300, 320 and 440 nm) in Fig. 5A, positioning arbitrarily the first point at zero. In B, a fresh sample was also submitted to the continuous preillumination, then dark deactivated for 20 s, illuminated by one flash, followed by another 20 s dark interval. Five detecting pulses were then triggered to determine a baseline, followed by a series of eight actinic flashes as in A, with a detecting pulse 50 ms after each flash. In procedure C, the preillumination sequence was: 1 s continuous beam, 20 s darkness, one flash, 20 s darkness, a group of three flashes (50 ms apart), 20 s darkness. From these data, one computes the absorption change caused by each flash, taking the difference between the absorbance recorded after and before the flash (or using the averaged baseline in the case of the first flash). It is such absorption increments that were plotted in all the other figures of the present paper where sequences are shown. Procedure A is designated to approach steady-state conditions with an equipartition of the S-states. Procedure B, on the other hand, should yield a maximal initial order of the system, by setting almost 100% of the centers in state S_1. Procedure C, should put about 60% of the centers in state S_0, the rest in S_1.

The data of Fig. 5 readily suggest the presence of – at least – two additional contributions superimposed on the S-related absorption changes. Let us first consider part A. There still remains a weak oscillatory pattern, suggesting that the equipartition of the S-states was not completely achieved, presumably because the intensity of the preillumination beam (and the corresponding rate of photochemical turnover) did not compete efficiently enough with the FCCP-accelerated deactivation of S_3 and S_2. Nevertheless, a good approximation of the steady-state absorption change can be obtained by averaging the increments on the eight flashes. The steady-state change expected for any signal related to the cyclical S-system is just zero, so that we have to recognize the presence of an extra steady-state signal, positive at 300 nm, negative at 320 nm. This signal (spectrum shown in Fig. 6C) is most probably assignable to the reduction of the plastoquinone acceptor pool which should proceed steadily upon each flash because of the equipartion of the two states of the two-electron gate Q_B. The purpose of experiment A is to measure this steady-state increment which will be subtracted from the other sequences. Another perturbation to the S-sequence is apparent from the data in B or C: the change of the first flash is anomalously large compared with the rest of the oscillating sequence. As will be discussed later, the amplitude of this first flash anomaly may vary to a significant extent depending on the algal culture, but its spectrum was reproducible.

Another interfering signal has to be taken into account, namely the cytochrome *b*-559 photooxidation catalyzed by FCCP. The experiments were run in the presence of a low concentration (500 nM) of this substance, so that only a small

fraction of cytochrome was oxidized at 50 ms after a flash. This oxidation was maximal after the first flash and then followed a rapidly damped period-4 oscillation. This maximal change was less than 6% of that obtained in the experiment of Fig. 2, that is about 4% of the total photooxidizable cytochrome. This means a quite small correction in the ultraviolet region, but it must be taken into account in the blue region around the Soret peak. In order to subtract the cytochrome signal, our experiments (of the type shown in Fig. 5) included a measurement at 559 nm, where it was checked that under similar conditions but in the absence of FCCP, negligible absorption change occurred. The 559 nm measurement obtained upon each flash was then used to weight the spectrum of Fig. 2 and subtract it from the data.

Fig. 6 shows a set of corrected spectra from experiments such as those of Fig. 5, except that only three flashes were fired in sequence B, which served as a preillumination for sequence C, without renewing the sample. This more compact procedure allowed a faster acquisition of the data, while the loss of information was found to cause no significant alteration of the deconvolution output, as shown in Table II (lines a and c). The spectra

TABLE II

CONTRIBUTIONS AT 320 nm OF TRANSITIONS $S_0 \rightarrow S_1$, $S_1 \rightarrow S_2$, $S_2 \rightarrow S_3$, AND FIRST FLASH ADDITIONAL COMPONENT (FF) OBTAINED FROM VARIOUS DECONVOLUTION PROCEDURES

Two sets of data obtained on different batches of algae were used, one in lines a–f, where two sequences of eight flashes were recorded following preilluminations of type B and C, and one in lines g–m, with only three flashes in the B sequence, eight in the C sequence. The first set was also used in Fig. 5, the second one in Figs. 6–8. The r.m.s. deviation between the predicted and experimental values for all flashes is given in column σ. The initial distribution for sequences B and C are given as, respectively, S_1 and S_1' ($S_0 = 1 - S_1$). a–e: α, β, S_1 and S_1' computed as described in the text (and Appendices). In a, the standard procedure was used, taking into account all 16 flashes, and treating *FF* as a fourth unknown present only on the first flash of B and C. In b, the contribution of *FF* on the first flash was taken as $(1 - \alpha)$, and α on the second flash. c is the same as a, but taking into account only the three first flashes of sequence B. d, same as a, but discarding the first flash of B and C, keeping only three unknowns; *FF* (given between brackets for B and C, respectively) was obtained by subtracting the predicted values from the experimental ones on the first flash. e, same as d, but using only sequence B. f: Ab initio deconvolution using a simplex method [32] with 29 free parameters as follow: (i) the value of S_1 after the continuous preillumination and deactivation (i.e., before the first preillumination flash); fitted value: 0.99; (ii) the values of α and β, that were not assumed to be identical on each transition; fitted values: $\alpha_0 = 0.10$, $\alpha_1 = 0.12$, $\alpha_2 = 0.088$, $\alpha_3 = 0.075$, $\beta_0 = 0.032$, $\beta_1 = 0.066$, $\beta_2 = 0.10$, $\beta_3 = 10^{-5}$; (iii) the spectral contributions of the three S-transitions and of the first flash component at five wavelengths (fitted values at 320 nm given in the table). Convergence achieved after 4000 iterations. The σ was computed on the 16 flashes at 320 nm. g–m: The sequence of type B consisted of three flashes, that of type C of eight flashes. In g, Kok's parameters were computed as described in the text. Different values of β were assayed in lines h and l, of α in j and k, of S_1 in l. m: Same deconvolution method as in f, using ten wavelengths. Convergence achieved after 4500 iterations. Fitted parameters: $S_1 = 0.96$ (after the continuous preillumination and deactivation); $\alpha_0 = 0.066$, $\alpha_1 = 0.116$, $\alpha_2 = 0.150$, $\alpha_3 = 0.108$, $\beta_0 = 0.058$, $\beta_1 = 0.081$, $\beta_2 = 10^{-5}$, $\beta_3 = 0.063$.

	$10^6 \cdot \frac{-\Delta I}{I}$								
	α	β	S_1	S_1'	S_0S_1	S_1S_2	S_2S_3	*FF*	σ
a	0.1	0.05	0.98	0.371	238	1622	1038	819	77
b	0.1	0.05	0.98	0.371	255	1636	950	894	77
c	0.1	0.05	0.98	0.371	113	1716	1054	796	63
d	0.1	0.05	0.98	0.371	297	1567	1066	(891, 773)	81
e	0.1	0.05	0.98	(0.371)	552	1360	1037	(1069, 704)	42
f		(.....see legend.....)			226	1562	1281	874	64
g	0.1	0.057	0.98	0.382	62	1492	1012	1096	38
h	0.1	0.057	0.98	0.355	168	1466	810	1124	64
i	0.1	0.04	0.98	0.418	−98	1494	1292	1074	54
j	0.08	0.057	0.98	0.345	26	1346	960	1204	62
k	0.13	0.057	0.98	0.436	122	1744	1060	918	36
l	0.1	0.057	0.90	0.423	−24	1666	1008	1040	52
m		(.....see legend.....)			112	1536	1002	1018	33

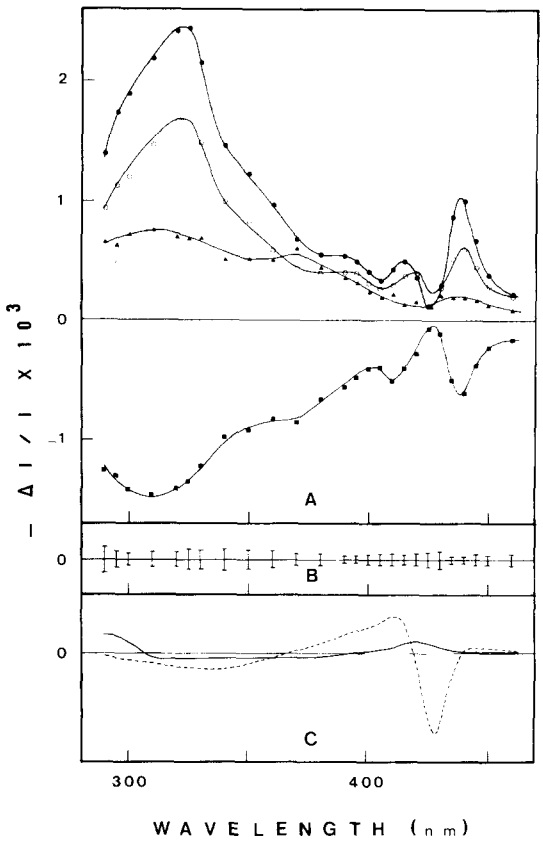

Fig. 6. (A) Spectra of the absorption changes induced by the first three flashes in sequence B (●, ▲, ■), and the first flash in sequence C (○). The data were corrected for the steady-state increment and cytochrome *b*-559 photooxidation as explained in the text. (B) Error bars for the spectra in A are indicated for each wavelength. (C) Spectrum of the steady-state increment (solid line) and maximum contribution (i.e., for the first flash of sequence B) of the cytochrome spectrum (dashed line). Same vertical scale in A, B, and C.

were obtained by (i) computing the increment caused by each flash (absorbance at flash n − absorbance at flash $n-1$); (ii) subtracting the averaged steady-state change obtained from procedure A; and (iii) subtracting the cytochrome signal as described above. Thus, no correction of the anomalous first flash signal was attempted at this step. The figure gives the spectra for the three flashes of sequence B, and for the first flash of C. We also plotted at the same scale (panel C) the spectra used in the subtractions, that of the steady-state increment, and that of the cytochrome at its maximal extent (first flash in B). The error bars indicated in panel B are meant for the corrected spectra, and were computed from the r.m.s. noise recorded on the baselines.

As stated above while discussing Fig. 4, the signal upon the first flash is lower after preillumination C (three flashes) than after preillumination B (one flash) in the range 290–400 nm, indicating a smaller $S_0 \rightarrow S_1$ absorption change compared with that of $S_1 \rightarrow S_2$ in this region. Other qualitative information that may be drawn from this figure is that the spectral shapes (correcting for the directions and amplitudes of the changes) obtained after two or three flashes are quite different in the blue region, indicating that there is more than one single spectral component corresponding to the S-transitions. The different spectrum on the first flash, on the other hand, is primarily due to the additional 'anomalous' component.

Deconvolution

The basic procedure we used may be outlined as follows.

(i) Determine Kok's parameters: α, β, and initial S_0/S_1 distributions for B- and C-type sequences. The weight of each transition $S_0 \rightarrow S_1$, $S_1 \rightarrow S_2$, $S_2 \rightarrow S_3$ is then computed for each flash.

(ii) Solve at each wavelength the linear system in which the spectral contributions of each transition are unknown, the weights of the transitions are coefficients, and the (corrected) absorption changes give the right-hand members. There are thus at each wavelength three unknowns and a number of equations equal to that of the flashes taken into account. A policy has to be adopted as to the first flash, that may be either discarded or taken into account, allowing then a fourth unknown for the additional first flash component.

The determination of Kok's parameters may be obtained by several methods. It is possible to use oxygen-evolution sequences and search the parameters that give the best fit. Similar sequences can be recorded spectrophotometrically by monitoring the 1 ms component of the absorption decay at 295 nm following each flash [12,13,17]. Such a procedure was used in Ref. 13. One can also use Lavorel's analysis [31] showing that the information about parameters α and β is fully present in sequence data for any linear combination of the S-states. The value of α and β can be retrieved by

solving a simple linear system. Thus, this method can be directly applied to the basic material that will be used for deconvolution of the S-spectra. We adopted this method because the signal-to-noise ratio is better in the S-related sequences than in the (spectrophotometrically derived) oxygen-type sequences. A large set of S-related sequences is available by taking the data obtained at various wavelengths according to procedures B or C (discarding the first flash). This method (see appendix) gave consistent results, yielding values of α between 0.10 and 0.12, and β close to 0.05.

The initial S_0/S_1 distribution may be predicted from the assumption of an equipartition of the S-states during the continuous illumination. This yields $S_0 = 0.25$ and $S_1 = 0.75$ after deactivation of S_2 and S_3. Then, taking into account the values of α and β, one obtains initial concentrations of $S_0 \approx 0.02$ and $S_1 \approx 0.98$ for sequence B. The initial S_0 for sequence C is then computed as that occurring after the third flash of sequence B (about 0.6), and S_1 taken as $1-S_0$. However, as apparent from Fig. 5A, the continuous preillumination does not cause complete equipartition because of the FCCP-accelerated deactivation, which should result in a concentration of S_0 somewhat lower than 25%. This is of no great consequence, however, since the initial S_1 in B must lie anyway between 0.98 and 1. Thus, the 0.98 estimate is reasonably safe. The set of Kok's parameters thus obtained gave quite satisfactory fit to the oxygen-type sequences (not shown).

The second step (ii) consists in solving an overdetermined linear system (more equations than unknowns), but where noise-affected data appear at the right-hand member (see Appendices). The standard procedure that we applied made simultaneous use of all the 16 (or 11, when using only a three-flashes sequence for B) flash data obtained at each wavelength following B and C preilluminations. Most of the useful information is present in the first few flashes, so that shorter sequences might have been used as well. However, since the estimation of α and β required – at least – eight flashes sequences, our policy was to use all the available data. The anomalous component on the first flash was treated as a fourth unknown, assumed to be present in equal amounts on the first flashes in B and C, and absent on the other flashes. The latter assumption (no additional contribution outside the first flash) may be somewhat approximate, but justified by the satisfactory agreement with Kok's model obtained under such conditions (see Fig. 8). Table II (line b) shows the effect of allowing a fraction of this component on the second flash as well. As to the assumption of equal amounts in sequences B and C, there is indeed no particular reason to believe that the three additional preillumination flashes in C should alter this contribution, considering that a prior multi-turnover preillumination, and a 20 s relaxation time after the flashes, were used in both cases. Fig. 4 supports this view, where the preillumination dependence of the first flash signal does not reveal any particular trend in addition of the effect of the S_0/S_1 initial distribution. Besides, when running the deconvolution without taking into account the first flashes (see Table II, lines d and e), the additional contributions present on the first flashes of sequences B and C can be separately computed and turn out to be reasonably close to each other. The reason for running simultaneously the deconvolution on both sequences, first flashes included, is that much useful information is contained in the first flash data of C concerning the $S_0 \rightarrow S_1$ transition (and the anomalous contribution as well), so that an improved overall accuracy may be expected. It should be mentioned, however, that running the deconvolution on the sole C sequence (first flash discarded), yielded erratic results. This turned out to be due to a basic indeterminacy when using this limited information: computed theoretical sequences also yielded erratic deconvolutions (but excellent fit) because very small computational errors caused large instabilities. This is a clear indication that the information that can be retrieved drops dramatically with the damping of the sequences. When the first flash is discarded, one still gets reliable deconvolutions if the initial distribution is close to 100% S_1, whereas the indeterminacy becomes total when $S_0 \approx S_1 \approx 50\%$. In Ref. 17, we similarly pointed the poor discriminative information contained in sequences starting with 25% S_0, 75%S_1, when the first flash cannot be used.

Fig. 7 shows typical output of our deconvolution procedure, using data from the same experiment as in Fig. 6. In regions where a compara-

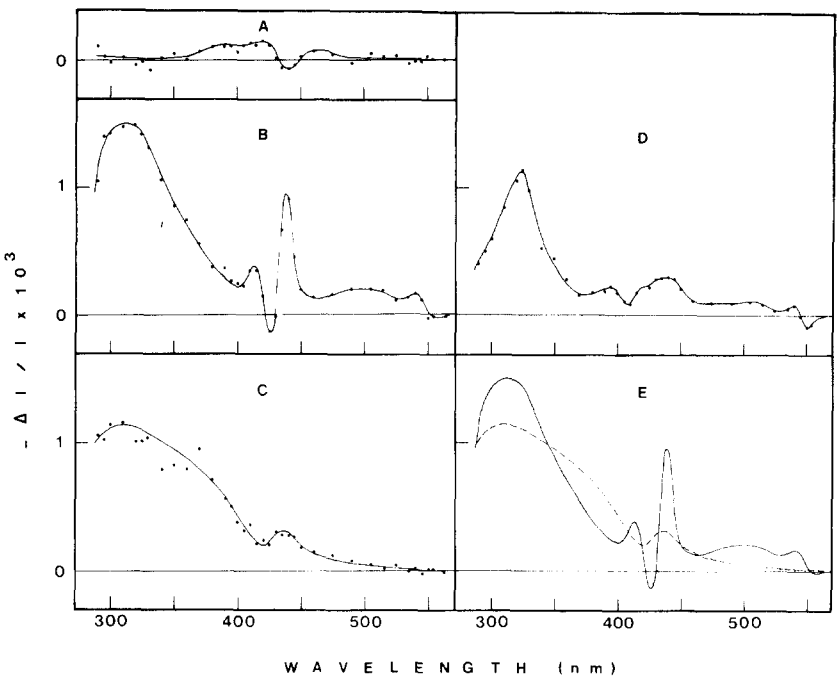

Fig. 7. Deconvoluted difference spectra for $S_0 \rightarrow S_1$ (A), $S_1 \rightarrow S_2$ (B), $S_2 \rightarrow S_3$ (C), and first flash additional component (D). In regions where the computed points are scattered (such as the ultraviolet region for the $S_2 \rightarrow S_3$ change), or too scarce (around 290 nm), the lines were drawn taking into account the results from other experiments. The spectra drawn in A, B, and C were replotted in E for comparison (dotted, solid and dashed lines, respectively). The data were taken from the same experiment as in Fig. 6. The deconvolution was run taking $\alpha = 0.1$, $\beta = 0.057$, $S_1 = 0.98$ for sequence B, from which $S_1 = 0.382$ was computed for sequence C.

tively large scatter of the points occurs, the lines were drawn taking into account information obtained from other experiments. Fig. 8 allows a comparison between the experimental data from Fig. 6 and the values computed from the spectra of Fig. 7: as may be seen, a satisfactory fit is obtained. Whereas both the spectral shapes and respective amplitudes for the S-transitions were obtained with a quite satisfactory reproducibility from a number of experiments, using slightly modified experimental or deconvolution procedures (as examplified in Table II), the amplitude of the first flash additional component was found to vary to a large extent in different batches of algae. Thus, the spectrum shown in Fig. 7D lies in the upper part of the amplitude range that was observed, while the lower part would be about twice smaller. The origin of this scatter does not seem to arise from fluctuations in the way the algae were collected and pretreated, and certainly not from the experimental and deconvolution procedure itself. Thus, the algal culture is likely to be involved although care was taken to proceed under well-defined conditions. In spite of the variable amplitude, the spectral shape was mostly reproducible, except for some fluctuations around 430 nm that will be discussed later.

As expected, the spectrum of the $S_0 \rightarrow S_1$ transition (Fig. 7A) has a small amplitude: it is actually close to the baseline in the ultraviolet, but the line drawn in the blue region is probably significant. The main difference in the spectra of $S_1 \rightarrow S_2$ and $S_2 \rightarrow S_3$ (see Fig. 7E) is observed in the blue region. The bandshift with positive peaks around 413 nm and 438 nm and negative peak around 425 nm belongs only, as a first approximation, to the $S_1 \rightarrow S_2$ change. In the 290–340 nm range, the $S_2 \rightarrow S_3$ spectrum is lower than that of $S_1 \rightarrow S_2$, and peaks at slightly shorter wavelength (305 nm instead of 315 nm, on average). Other differences are observed in the green region, where the $S_1 \rightarrow S_2$ change is predominant.

The features described above were consistently obtained from a number of experiments, using

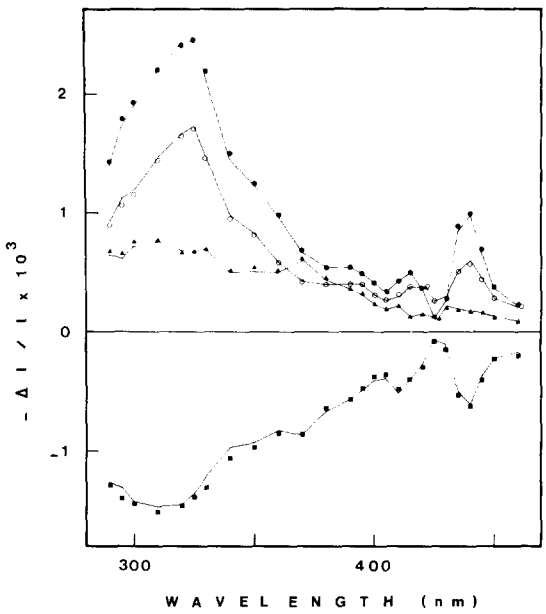

Fig. 8. Fitting of the data of Fig. 6, using the deconvoluted spectra of Fig. 7. The symbols indicate the computed values (●, ▲, ■ for the three flashes of B in their respective order, ○ for the first flash of C). The straight lines were drawn joining the experimental points taken from Fig. 6. Examples of the standard deviation computed on all (11) flashes may be found in Table II.

slightly different experimental and deconvolution procedures. Table II shows that reasonable variations in the deconvolution parameters do not affect the output dramatically. Also given in this table (lines f and m) are results obtained from a completely ab initio method using a simplex routine [32]. In this case, in addition to the four spectral components to be determined at each wavelength, the program takes as free parameters the S_0/S_1 distribution before the preillumination flashes, and four couples of values for α and β, accepting that these parameters may vary according to each S-state (see the review Ref. 33). A satisfactory convergence is obtained after a few thousands iterations (remember that if ten wavelengths are taken into account, the program has to fit 49 parameters), and the results that turn up are close to those obtained using our standard procedure. The differences in the α's and β's that come out are probably not significant as no consistent pattern was obtained. The main interest of this ab initio fitting is to confirm that there is no particular bias or instability in the standard deconvolution procedure we used.

Discussion

A critical point in studying S-related absorption spectra is the elimination of the two-flash periodic change associated with Q_B. The technique we used takes advantage of the FCCP action which uncouples the S-states deactivation from Q_B^- reoxidation. On the other hand, it was checked that, under the conditions we used, FCCP did not modify significantly the S- and Q_B-sequences observed with fully dark-adapted material. The additional photooxidation of a small fraction of cytochrome *b*-559 can be easily corrected. By using suitable preillumination procedures we obtained data free from any Q_B/Q_B^- contribution, a point that is bound to make the deconvolution simpler and more reliable.

The main conclusion from the present work is that, in contradiction with previous reports [13,30], the three observable S-transitions have different spectra in the near ultraviolet and visible regions. The $S_0 \rightarrow S_1$ step causes only a very small absorption change. The $S_1 \rightarrow S_2$ spectrum is similar with that reported by Dekker et al. [34] with a broad peak around 315 nm, and a bandshift in the blue region, superimposed on the tail of the main band. As suggested in Ref. 13, this shift is most probably that of a Chl *a* spectrum, perhaps P-680. The occurrence of this electrochromic effect on transition $S_1 \rightarrow S_2$, and, as a first approximation, on this transition only, is consistent with the 1,0,1,2-pattern for proton release [7–9], which implies [12] that the net charge of the system does not change during the $S_0 \rightarrow S_1$ or $S_2 \rightarrow S_3$ steps, but is increased by one unit during the $S_1 \rightarrow S_2$ step. The presence of a positive net charge on the oxygen-evolving complex causes a shift of the Chl *a* blue absorption band towards longer wavelengths, whereas an opposite shift was reported in the red region [14]. A quantum-mechanical prediction of such shift directions was given in Ref. 35.

This bandshift is mostly absent from the $S_2 \rightarrow S_3$ spectrum, although there seems to be a small contribution which may be a deconvolution artefact. It is not unlikely, however, that in spite

of the net charge conservation on this step, local charge effects might still occur. The $S_2 \rightarrow S_3$ spectrum is also different from that of $S_1 \rightarrow S_2$ in the ultraviolet where it is smaller and peaks at a shorter wavelength (305 nm). We do not view this latter feature as being as solidly established as the previous ones, which emerge almost directly from the experimental data, whereas in this case it mostly comes out of the deconvolution. Nevertheless, we believe it to be significant, because it was very consistently obtained using various experimental and deconvolution procedures.

In a previous paper [17], I reported semi-qualitative evidence suggesting that, if a unique spectral shape were associated with the various S-transitions, its amplitude was significantly smaller upon $S_0 \rightarrow S_1$ and $S_2 \rightarrow S_3$ than $S_1 \rightarrow S_2$. In terms of integer stoichiometries this led to support a 0,1,0,−1-pattern for manganese oxidation. The quantitative analysis of the present paper fully confirms the view of a very small ultraviolet change upon $S_0 \rightarrow S_1$, but shows that the change associated with $S_2 \rightarrow S_3$ is only slightly smaller than that of $S_1 \rightarrow S_2$. As far as the spectra of these transitions may be ascribed to identical species, the best integer stoichiometry would actually be 0,1,1,−2.

Up to now, three groups have published reports about the spectra of the S-transitions. The spectra proposed by Renger and Weiss [36] are obviously heavily contaminated with semiquinone binary oscillations, as now recognized by the authors [37]. Dekker et al. [13] have put forward the view of a unique difference spectrum in the ultraviolet with an identical amplitude on each transition (1,1,1,−3-model). We believe the problem here does not arise from the data but from the deconvolution procedure. The basic material used by these authors was corrected from the steady-state change, but contained a secondary-acceptor binary oscillation. To deconvolute the S-states spectra, they used a self-consistent procedure based on the assumptions of a unique spectral component occurring with a 1,1,1,−3-stoichiometry. From the uniqueness of the acceptor spectrum which emerged and from the similarity of the deconvoluted S-spectrum with that obtained in a one-flash experiment run in the presence of DCMU, the correctness of the assumptions was infered. Two objections may be raised, first as to the discriminative power of this method, second, as to its treatment of the secondary acceptor changes. As discussed earlier, it turns out that the retrieval of the individual spectra for each transition becomes rapidly impossible as soon as the initial distribution of the S-states is not sharply contrasted. The material used by Dekker et al. consisted of sequences with initial distribution of 25% S_0, 75% S_1, where the first flash is discarded. Independently of any other source of error (estimation of Kok's parameters, experimental accuracy, etc.), this blured initial situation has little discriminative power. Such considerations led us to design experiments where the initial concentration of S_1 was close to 100%, and to use the information present in the first flash using both this initial distribution and another one where the concentration of S_0 was made as high as possible. Another crucial point is the deconvolution of the secondary-acceptor signals. The way this is done in the work of Dekker et al. is bound to eliminate any change which appears and disappears alternatingly in the difference spectra of the successive S-states, as emphasized by the authors. This is actually what happens in the 320 nm region and in the 440 nm region, where the $S_0 \rightarrow S_1$ spectrum is low, the $S_1 \rightarrow S_2$ spectrum large, the $S_2 \rightarrow S_3$ spectrum lower again. The unique spectrum found for each S-transition using such a procedure is actually some average of three different spectra.

Saygin and Witt [30] also criticized Dekker et al.'s spectra, pointing out that little useful information on the $S_0 \rightarrow S_1$ transition is present in the data obtained under their experimental conditions. They attempted to measure the $S_0 \rightarrow S_1$ spectrum as that obtained upon the second flash in the presence of a low (25 μm) concentration of hydroxylamine. Under such conditions the oxygen-evolution, or other S-related sequences, are delayed by two flashes [38]. Saygin and Witt assumed that hydroxylamine reduced the S_1 centers to S_0 in the dark, and that the first flash caused hydroxylamine oxidation. The system would be thus initialized with about 100% S_0 before the second flash. The spectrum obtained under these conditions has a peak around 300 nm, where it is higher than the $S_1 \rightarrow S_2$ or $S_2 \rightarrow S_3$ spectra. This is in contradiction with our finding of very small absorption changes associated with this transition,

a point that readily emerges from the preillumination effects of Fig. 4. It thus seems likely that something is wrong with the assumptions of the authors concerning the mechanism of hydroxylamine action. For the two other transitions, the authors proposed identical spectra peaking around 340 nm, but the problem there may be the experimental accuracy.

The interpretation of the ultraviolet spectra in terms of manganese transitions is not straightforward. The changes observed in this region with synthetic Mn compounds [16,39] are due to ligand-to-metal charge-transfer bands [40], the energy of which depend both on the ligand and on the oxidation state of the metal. The transition is expected to decrease in energy as the oxidation state of the metal increases for a given ligand, and as the ionisation potential of the ligand decreases for a given state of the metal. Thus, ultraviolet bands similar with that observed for $S_1 \rightarrow S_2$ or $S_2 \rightarrow S_3$ have been reported both for the Mn(III $\rightarrow$ IV) oxidation in a binuclear Mn gluconate complex [16], and for the Mn(II $\rightarrow$ III) oxidation in oxo-bridged binuclear carboxylate complexes [39]. In the latter case, the Mn(II $\rightarrow$ III) transition gave a difference spectrum peaking around 305 nm, whereas the same transition in the gluconate system gave a peak around 240 nm. As to the spectra of the S-state transitions, one can thus put forward the following conclusions. For $S_0 \rightarrow S_1$, an Mn(III $\rightarrow$ IV) transition is unlikely, but an Mn(II $\rightarrow$ III) transition cannot be ruled out (if its ultraviolet band were present at shorter wavelengths than investigated here). Still, the most likely possibility is that no Mn oxidation is involved at this step. $S_1 \rightarrow S_2$ and $S_2 \rightarrow S_3$ may both correspond to Mn(II $\rightarrow$ III) or Mn(III $\rightarrow$ IV) oxidations, depending on the Mn ligands. Much of the presently available evidence from other techniques is consistent with, or suggests that $S_1 \rightarrow S_2$ is an Mn (III $\rightarrow$ IV) transition [2,3]. However, the occurrence of approximately similar ultraviolet bands for $S_1 \rightarrow S_2$ and $S_2 \rightarrow S_3$ does not imply that the same Mn transition is involved in both cases.

An interesting finding is the presence of a new photo-induced signal specifically present on the first flash of a series. Dekker et al. [13], using PS II particles, reported the occurrence of an anomalous change on the first flash with respect to the S- or Q_B-signals. This component turned out to be also present in algae, where we obtained its spectrum as a by-product of the deconvolution of the S-state spectra. The turnover time for this component is about a few seconds, since it is regenerated in less than 10 s, but not in the 100 ms time-range of the flashing interval. Preliminary experiments suggest that it is also present in the absence of FCCP, and also in the absence of quinone-treatment of the algae. When running the experiments in the absence of ionophore, so that some membrane potential was still present when the flash-induced change was sampled, the spectrum obtained for the additional first flash component was combined with the field-indicating absorption change, which shows that it corresponds to a photochemical reaction with normal electrogenic character (on the other hand, undistorted spectra for the S-transitions were still obtained, since the steady-state change subtraction properly eliminates the field-indicating change in this case). The relative extent of the additional change on the first flash, compared with the S-signals, was found variable with different batches of algae, although a consistent spectral shape was obtained. The shape of this spectrum in the ultraviolet is compatible with a transition $S_1Q_A \rightarrow S_2Q_A^-$. The bandshift in the 540–550 nm region also suggests the presence of Q_A^-. However, the fit is poor in the blue region. For instance, at 430 nm, a positive change was obtained (Fig. 7D), whereas the $S_1 \rightarrow S_2$ spectrum is isobestic, and that of $Q_A^- - Q_A$ slightly negative [20]. In other experiments we sometimes obtained a trough in this region, but never the expected negative change. However, 430 nm is close to the Soret peak of cytochrome *b*-559 so that the deconvolution output at this wavelength is sensitive to errors in the cytochrome correction. It is thus difficult to assign unambiguously this absorption change to centers with a blocked or slower electron transfer between Q_A and Q_B, but otherwise normal. The possibility remains of an acceptor with a different spectrum in the blue region. On the other hand, it may be noticed that the involvement of the secondary donor Z instead of S_1, as would be the case if centers with a deficient oxigen-evolving system were present (as in Tris-washed chloroplasts), is still harder to accommodate, since the 430–440 nm bandshift is larger, and

more negative at 430 nm in the $Z \rightarrow Z^+$ spectrum than for $S_1 \rightarrow S_2$ [34,41,20]. There have been many reports in the literature that may be put together with the signal discussed here. Among these are several proposals concerning a heterogeneity of PS II centers (see Ref. 42 for a review). Evidence for a reversible, pH-dependent state of PS II centers, with a slow Q_A^- reoxidation, was found by Diner and Joliot [43]. There are also recent reports that a significant part of the 320 nm change and of the field-indicating change obtained when using dark-adapted material is not attributable to normal centers as characterized through their oxygen-evolution and plastoquinone-reduction properties, but involves centers with a slower turnover [44,45].

Appendix A. Determination of α and β from the absorption change sequences

As shown by Lavorel (Eqn. 9 in Ref. 31), the following equation can be derived from Kok's model:

$$(Y_{n+4} - Y_n) - \sigma_1(Y_{n+3} - Y_n) + \sigma_2(Y_{n+2} - Y_n) - \sigma_3(Y_{n+1} - Y_n) = 0 \quad (1)$$

where Y_i is any linear combination of the concentrations of the S-states at flash i. In the usually considered case where α and β are assumed to be constant for all transitions, one has:

$$\sigma_1 = 4\alpha$$
$$\sigma_2 = 6\alpha^2 - 2\beta^2$$
$$\sigma_3 = 4[\alpha^3 - \alpha\beta^2 + \beta(1-\alpha-\beta)^2]$$

Our routine is a simplex fitting [32] of parameters α and β where the function to be minimized is $\sum L^2$, with L standing for the left-hand member of Eqn. 1. The summation is run over sequences of type B and C, over the data at all wavelengths except those where the signal-to-noise ratio is poor, and over all available flashes except the first one (thus, $1 < n < 4$).

Appendix B. Deconvolution of the S difference spectra

Parameters α and β were determined as described above, and the initial S_0/S_1 distributions for sequences B and C as explained in the text. One then computes the concentrations $S_i(n)$ following each flash n, with $i = 0$ to 3 and $n = 0$ to 8 for sequences B and C (assuming sequence B to consist of eight flashes). The contribution of each transition upon each flash is then obtained, using:

$$T_0(n) = (1-\alpha)S_0(n-1) - \beta S_2(n-1) - (1-\alpha-\beta)S_3(n-1)$$
$$T_1(n) = \beta S_0(n-1) + (1-\alpha)S_1(n-1) - \beta S_2(n-1) - (1-\alpha)S_3(n-1)$$
$$T_2(n) = \beta S_1(n-1) + (1-\alpha-\beta)S_2(n-1) - (1-\alpha)S_3(n-1)$$

where $T_i(n)$ is the contribution of transition $S_i \rightarrow S_{i+1}$ upon flash n. These equations were derived taking into account the equivalence of the $S_3 \rightarrow S_0$ transition with: $-(S_0 \rightarrow S_1 + S_1 \rightarrow S_2 + S_2 \rightarrow S_3)$. One considers also the transition weight $T_4(n)$ for the additional component on the first flash, taking $T_4(1) = 1$ and $T_4(n) = 0$ for $n \neq 1$. Denoting the difference spectrum for each transition by $S_iS_{i+1}(\lambda)$ and $FF(\lambda)$ for the additional first flash component, one has, for each flash n, the equation:

$$\sum_{i=1}^{3} T_i(n) S_iS_{i+1}(\lambda) + T_4(n) FF(\lambda) = A_n(\lambda) \quad (2)$$

where $A_n(\lambda)$ is the experimental absorbance change corrected as explained in the text. Thus, Eqn. 2 gives, for each λ, a linear system of 16 equations (when the 8-flash data of sequences B and C are used) with four unknowns. The system cannot, however, be solved exactly, since the A_n values are error-affected data. One thus considers the 16-dimensional vector-space where each dimension stands for a flash number, and the manifold determined by the four vectors with components $T_i(n)$ ($i = 1$ to 4). An orthogonal basis is computed for this subspace using Schmidt's orthogonalization method. The projection on this manifold, and distance D from it, of the vector with components A_n is then easily obtained. This distance D rates the quality of the deconvolution, expressing how closely the experimental values may be fitted with the assumed model. The σ value given in Table II is $D/\{(\text{number of flashes})^{1/2}\}$. The projected vector is an exact solution of the over-determined linear system. The system is solved, keeping four equations, selected

with a pivot method for minimizing computational errors.

References

1 Kok, B., Forbush, B. and McGloin, M. (1970) Photochem. Photobiol. 11, 457–475
2 Dismukes, G.C. (1986) Photochem. Photobiol. 43, 99–115
3 Govindjee, Kambara, T. and Coleman, W. (1985) Photochem. Photobiol. 43, 187–210
4 Vermaas, W.F.J., Renger, G. and Dohnt, G. (1984) Biochim. Biophys. Acta 764, 194–202
5 De Groot, A., Plijter, J.J., Evelo, R., Babcock, G.T. and Hoff, A.J. (1986) Biochim. Biophys. Acta 848, 8–15
6 Bouges-Bocquet, B. (1973) Biochim. Biophys. Acta 292, 772–785
7 Fowler, C.F. (1977) Biochim. Biophys. Acta 462, 414–421
8 Saphon, S. and Crofts, A.R. (1977) Z. Naturforsch, 32c, 617–626
9 Förster, V. and Junge, W. (1985) Photochem. Photobiol. 41, 183–190
10 Dismukes, G.C. and Siderer, Y. (1981) Proc. Natl. Acad. Sci. USA 78, 274–278
11 Pulles, M.P.J., Van Gorkom, H.J. and Willemsen, J.G. (1976) Biochim. Biophys. Acta 449, 536–540
12 Velthuys, B.R. (1981) in Photosynthesis II (Akoyunoglou, G., ed.), pp. 75–85, Balaban International Science Services, Philadelphia, PA
13 Dekker, J.P., Van Gorkom, H.J., Wensink, J. and Ouwehand, L. (1984) Biochim. Biophys. Acta 757, 1–9
14 Saygin, O. and Witt, H.T. (1985), FEBS Lett. 187, 224–226
15 Dismukes, G.C. and Mathis, P. (1984) FEBS Lett. 178, 51–54
16 Bodini, M.E., Willis, L.A., Riechel, T.L. and Sawyer, D.T. (1976) Inorg. Chem. 15, 1538–1543
17 Lavergne, J. (1986) Photochem. Photobiol. 43, 311–317
18 Renger, G. (1978) in Proceedings of the IInd International Congress on Photosynthesis Research (Forti, G., Avron, M. and Melandri, A., eds.), Vol. I, pp. 53–60, Junk, Dordrecht
19 Lacambra, M., Larsen, U., Olive, J., Bennoun, P. and Wollman, F.A. (1984) Photobiochem. Photobiophys. 8, 191–205
20 Lavergne, J. (1984), FEBS Lett. 173, 9–14
21 Lavergne, J., Delosme, R., Larsen, U. and Bennoun, P. (1984) Photobiochem. Photobiophys. 8, 207–219
22 Ovchinnikov, Yu, A., Ivanov, V.T., and Skrob, A.M. (1974) Membrane Active Complexones, Elsevier, Amsterdam
23 Joliot, P., Béal, D. and Frilley, B. (1980) J. Chim. Phys. 77, 209–216
24 Joliot, P. and Joliot, A. (1984) Biochim. Biophys. Acta 765, 210–218
25 Lavergne, J. and Etienne, A.L. in Proceedings of Vth International Congress on Photosynthesis (Akoyunoglou, G., ed.), Vol. III, pp 939–948, Balaban International Science Services, Philadelphia, PA
26 Hanssum, B., Dohnt, G. and Renger, G. (1985) Biochim. Biophys. Acta 806, 210–220
27 Ben-Hayym, G. (1972) FEBS Lett. 28, 145–149
28 Garewal, H.S. and Wasserman, A.R. (1974) Biochemistry 13, 4063–4071
29 Pulles, M.P.J., van Gorkom, H.J. and Verschoor, G.A.M. (1976) Biochim. Biophys. Acta 440, 98–106
30 Saygin, O. and Witt, H.T. (1987) in Progress in Photosynthesis Research (Biggins, J., ed.), Vol. I, pp. 537–540, Martinus Nijhoff, Dordrecht
31 Lavorel, J. (1978) J. Theor. Biol. 57, 171–185
32 Nelder, J.A. and Mead, R. (1965) Computer J. 8, 308–313
33 Bouges-Bocquet, B. (1980) Biochim. Biophys. Acta 594, 85–103
34 Dekker, J.P., Van Gorkom, H.J., Brok, M. and Ouwehand, L. (1984) Biochim. Biophys. Acta 764, 301–309
35 Pancoska, P., Kapoun, M. and Skala, L. (1983) Photobiochem. Photobiophys. 6, 39–46
36 Renger, G. and Weiss, W. (1986) Biochim. Biophys. Acta 850, 184–196
37 Renger, G., Hanssum, B. and Weiss, W. (1987) in Progress in Photosynthesis Research (Biggins, J., ed.), Vol. I, pp. 541–544, Martinus Nijhoff, Dordrecht
38 Bouges, B. (1971) Biochim. Biophys. Acta 234, 103–112
39 Vincent, J.B. and Christou, G. (1986) FEBS Lett. 207, 250–252
40 Cotton, F.A. and Wilkinson, G. (1980) in Advanced Inorganic Chemistry, Wiley, New-York
41 Diner, B.A. and De Vitry, C. (1984) in Advances in Photosynthesis Research (Sybesma, C., ed.), Vol. I, pp. 407–411, Martinus Nijhoff/Dr.W. Junk Publishers, Dordrecht
42 Black, M.T., Brearley, T.H. and Horton, P. (1986) Photosynthesis Research 8, 193–207
43 Diner, B. and Joliot, P. (1976) Biochim. Biophys. Acta 423, 479–498
44 Chylla, R., Garab, G. and Whitmarsh, J. (1987) in Progress in Photosynthesis Research (Biggins, J., ed.), Vol. II, pp. 237–240, Martinus Nijhoff, Dordrecht
45 Graan, T. and Ort, D.R. (1987) in Progress in Photosynthesis Research (Biggins, J., ed.), Vol. II, pp. 241–244, Martinus Nijhoff, Dordrecht